Smartphones and Gravitational Acceleration II: Applications

Cite as: Phys. Teach. **58**, 473 (2020); https://doi.org/10.1119/10.0002064
Published Online: 23 September 2020

Meryem Berrada, Joshua A.H. Littleton, and Richard Secco

Smartphones and Gravitational Acceleration II: Applications

Meryem Berrada, Joshua A. H. Littleton, and Richard Secco, University of Western Ontario, London, ON, Canada

The exercises described here conveniently exploit the built-in acceleration sensors in smartphones, devices that are becoming ubiquitous if not essential items for most students. This allows each student to have the opportunity for a hands-on experience and to collect their own data, reduces preparation time, and greatly reduces cost by removing the need of purchasing a gravimeter to perform the same or similar tasks in gravity surveys. These exercises further demonstrate the educational value of using smartphones as scientific tools and that freely available accelerometer software applications operate with acceptable tolerance. The differences between accelerometers placed in smartphones and gravimeters are further discussed in the companion paper, "Part 1: Smartphone Applications for Gravitational Acceleration Surveys."[1]

Gravitational acceleration factors and corrections: Latitude and elevation

In conducting a gravity survey, it is important to be aware of all accelerations that could affect the measurement. Since an accelerometer used in the survey records acceleration, it will record any acceleration it experiences, regardless of whether the force that causes the acceleration is due to Earth's gravitational field or any other force. For example, if an acceleration measurement was taken in an elevator as it is beginning to accelerate upwards, the device would record a value larger than a_{grav}. It is therefore imperative to be aware of unwanted acceleration contributions and how to account for these when designing a survey. A full demonstration of gravity processing would require more data and time than is normally scheduled in a laboratory exercise at the junior post-secondary level. The exercise described here will concentrate on two main effects: i) effects due to Earth's rotation; and ii) effects due to height above mean sea level.

Since Earth is spinning about its rotation axis, centrifugal force is maximum at the equator and zero at the poles. As such, measurements of gravitational acceleration (a_{grav}) at the equator show a lower value than at the poles. In other words, a_{grav} varies as a function of latitude. Similarly, if two measurements of a_{grav} are taken at the exact same location but differ only in height above mean sea level (elevation), the measurements will be different. The measurement at the higher elevation will be lower due to the inverse-square dependence of the gravitational force on the distance to the center of Earth as given in Newton's first law of gravitation. Typically, all gravity survey measurements are adjusted so that they are compared at some reference elevation. A simple theoretical value of local a_{grav} can be calculated using the following:

$$a_{theory} = a_{lat} + a_{el}\,, \tag{1}$$

where a_{theory} is the calculated theoretical value of local gravitational acceleration, a_{lat} is the latitude-dependent contribution to the gravitational acceleration, and a_{el} is the elevation-dependent contribution to the gravitational acceleration. The a_{lat} term is further defined by the 1980 International Gravity Formula[2] as follows:

$$a_{lat} = 9.780327\cdot(1+0.0053024\cdot\sin^2\varphi - 0.0000058\cdot\sin^2 2\varphi)\,, \tag{2}$$

where φ is latitude in degrees and a_{lat} is in units of m/s^2. Similarly, the a_{el} term is further defined by the elevation (also known as free-air) correction approximation as follows:

$$a_{el} = (-3.086\times10^{-6})\cdot h\,, \tag{3}$$

where h is height or elevation above mean sea level in meters and a_{el} is in units of m/s^2. Mean sea level is chosen as the reference elevation because it coincides with the theoretical equipotential surface of Earth's gravity field. The true equipotential gravitational surface is called the geoid, while the best mathematical fit of this highly undulated surface is called the reference ellipsoid. Thus, it is more precise to say φ and h represent the latitude and height with respect to the reference ellipsoid, as illustrated in Fig. 1. Heights or elevations below the reference ellipsoid are to be input as a negative value. Derivations of Eqs. (2) and (3), along with other more sophisticated models intended for highly specialized applications, are outside the scope of this paper and can be found in numerous sources elsewhere.[3-6]

There are other factors not taken into account for this exercise but should be mentioned. For instance, the gravitational fields of the Moon and Sun exert forces on Earth, and the changes in Earth shape that these forces cause, as in the

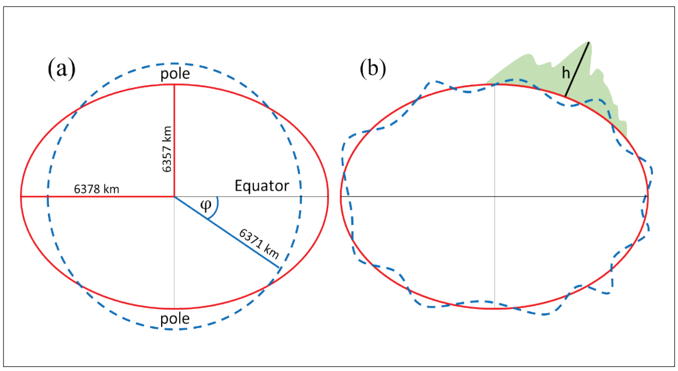

Fig. 1. (a) Illustration of a cross section of the theoretical equipotential surface (blue dashed line) compared to the reference ellipsoid (red line). The radius of the theoretical surface is approximately 6371 km. The minor radius of the reference ellipsoid is 6357 km, while the major radius is 6378 km. The latitude angle φ is defined as the angle between the equator and the location on the theoretical surface. (b) Illustration of the reference ellipsoid (red line) compared to the geoid (blue dashed line), Earth's actual gravitational equipotential surface, and the topography (green shaded area). The distance between a point on the topographic high and the reference ellipsoid is *h*.

liquid and solid Earth tides, occur slowly over the course of a day. In order to correct for this, base-station readings and a drift correction must be performed and implemented. In short, this involves returning to the same location throughout the survey periodically, known as a base station, to repeat measurements in order to measure how a_{grav} varies with time. The variation in a_{grav} can be a combination of several sources such as the liquid or solid Earth tides and the reproducibility of the instrument. These base station measurements can then be used to correct the survey measurements (called a drift correction) to remove some of the effects of the time variations. Lastly, if the interest is purely for investigating density contrasts, a gravity survey can be ruined simply because of a few topographic variations. For instance, measurements taken at the peak of a mountain can differ considerably from those taken at the same elevation but far away from the mountain, such as in an airplane. This difference is because there is a much larger density (i.e., the mountain rocks) between the mountain peak measurements and the reference ellipsoid. In order to correct for the effect that variations in landscape elevation, or topography, has on the survey, a Bouguer correction is applied.[4] This correction removes the effect of excess mass caused by the mountain peak to leave only density contrasts at mean sea level between a buried body and the average sub-surface crustal rocks. The applications used in this exercise simply measure the device motion at any fixed latitude and elevation and do not correct the acceleration for the factors discussed above.

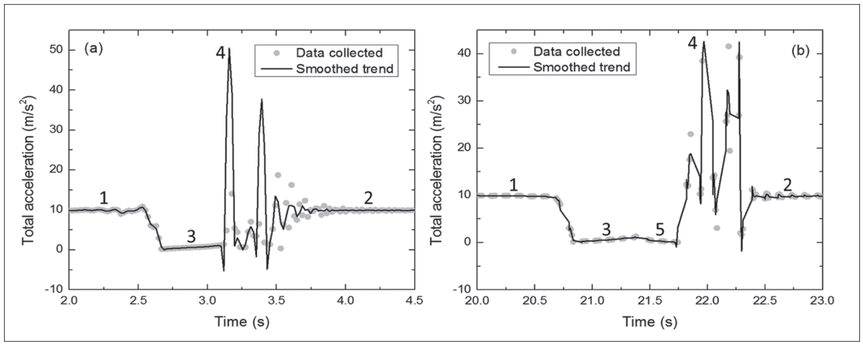

Fig. 2. Results of the free fall exercise conducted using (a) GraphicalGW and (b) Physics Toolbox Sensor Suite applications. Shown are the total acceleration magnitudes vs. time. The left- and right-most horizontal trends (regions 1 and 2) in both plots indicate when the smartphone device was stationary. Conversely, in both plots, the horizontal trend (region 3) at approximately 0 m/s^2 indicates when the smartphone device was in free fall. The large peaks after the free fall trend (peak 4) indicate when the smartphone device contacted and bounced on a cushion. (b) shows a deviation (region 5) from the 0 m/s^2 trend during free fall that indicates rotation of the smartphone (i.e., a rotation of the *z*-axis away from the true vertical).

Gravity-related exercise: Determination of local a_{grav} via free fall

The purpose of this exercise is to determine experimentally the magnitude of local a_{grav} using a smartphone device and accelerometer software application and compare it to the calculated a_{theory} using Eqs. (1)-(3). The smartphone device should be held with the *z*-component axis oriented normal to, and at some distance above, the floor. The device is released from the student's grasp and should land on a soft object, such as a pillow or cushion, to absorb the impact. The students are encouraged to be mindful of the fact that the release of the smartphone should not impart any additional force to the phone (e.g., pushing the device down). This is not difficult to control so it should only contribute negligible error to the data. During free fall, both applications record 0 m/s^2. While GraphicalGW already displays values in m/s^2, the *g*-force ratio of 0 recorded in Physics Toolbox Sensor Suite comes from the measured F_N of 0 N. Conversely, while the smartphone is stationary, the ratio is equal to unity.

Figure 2 depicts the results of the free fall exercise for GraphicalGW [Fig. 2(a)] and Physics Toolbox Sensor Suite [Fig. 2(b)]. After timing began and the smartphone was being held stationary above a cushion, both figures show a constant acceleration of approximately 9.8 m/s^2, equivalent to a *g*-force ratio of unity. Following this trend is a rather abrupt drop that stabilizes to establish a second horizontal trend with values of acceleration of approximately 0 m/s^2 corresponding to a *g*-force ratio of 0. This observed signal indicates the smartphone was released and is in free fall. The slight increase of total acceleration observed while in free fall can be explained by minor rotations of the smartphone device after release. While rotating, the *z*-axis of the accelerometer moves off vertical and thus does not provide reliable data. For this reason, only the first data point of the free fall phase should be considered. The largest peaks following the free fall trend indicate when the smartphone landed and bounced on the cushion. The smartphone eventually came to rest on the cushion, and the trend returns to a similar state prior to the release.

To incorporate elementary physical measurement procedure, students should select several measurements, or as many as reasonably possible, and average them to determine a single quantity to best represent the magnitude of acceleration of the smartphone both prior to and during free fall. In our case, all measurements up to two seconds prior to free fall were selected and averaged over 10 experimental runs to calculate the magnitude of acceleration of the smartphone prior to free fall. Similarly, the first measurement of the free fall phase of 10 experimental runs were averaged to calculate the magnitude of acceleration of the smartphone during free fall. Using the same selected data, the students are also encouraged to calculate the standard deviation to determine uncertainty in the quantities. The difference between the two values will give the experimentally determined magnitude of local a_{grav}:

$$a_{grav} = a_{ptf} - a_{df}, \tag{4}$$

where a_{ptf} is the average magnitude of acceleration prior to free fall (ptf) and a_{df} is the average magnitude of acceleration during free fall (df). The resultant uncertainty of a_{grav} can be calculated using elementary uncertainty propagation:

$$\sigma_{grav} = \sqrt{\sigma_{ptf}{}^2 + \sigma_{df}{}^2}, \tag{5}$$

where σ_{grav} is the uncertainty of a_{grav}, and σ_{ptf} and σ_{df} are the standard deviations of a_{ptf} and a_{df}, respectively. The students must look up, or be provided with by the instructor, the latitude and height above mean sea level of their location. Students then use Eqs. (1)-(3) to calculate a_{theory}. For simplicity, we assume no error in latitude or height. Our location has a latitude of approximately 43°N and a height above sea level of approximately 251 m. The measured gravitational acceleration a_{grav} can be compared to the theoretical value, a_{theory}. Our results are given in Table I.

Students should be asked to discuss potential sources of error and/or measurement bias that may have contributed to any observed difference between experiment and theory. The simplicity of the exercise combined with the accessibility of free software applications means that it is possible to have every student conduct and collect their own data and analysis using their own smartphone.

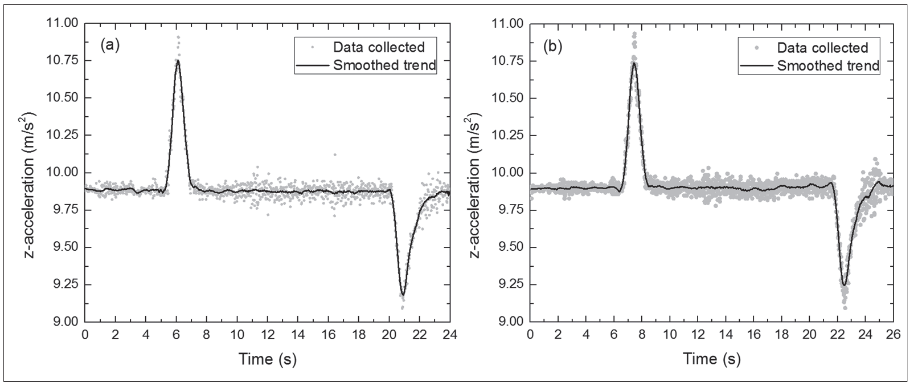

Fig. 3. Results of the elevator exercise conducted using (a) GraphicalGW and (b) Physics Toolbox Sensor Suite applications. Shown are the magnitudes of the *z*-component of the total acceleration versus time. The left-most peak and right-most trough represent the elevator accelerating and braking, respectively. While stationary, before the peak, or traveling at a constant velocity, after the peak and before the trough, the elevator shows no acceleration.

Table I. Results of the free fall exercise using GraphicalGW and Physics Toolbox Sensor Suite on a smartphone device.

Application	a_{ptf} (m/s^2)	a_{df} (m/s^2)	a_{grav} (m/s^2)	a_{theory} (m/s^2)
GraphicalGW	9.91 ± 0.08	0.14 ± 0.02	9.77 ± 0.08	9.81
Physics Toolbox Sensor Suite	9.9 ± 0.1	0.15 ± 0.01	9.8 ± 0.1	

Mechanics-related exercise: Determination of elevator acceleration

Classrooms do not normally contain materials with sufficiently large density contrast and size or have the physical dimensions with associated variations in elevation or latitude that would have noticeable effect on local a_{grav}. However, a possible solution for an additional exercise with measurable effects is to carry out an acceleration survey inside an elevator. Different types of elevators exist for different purposes and each has different operational travel velocities, ascending accelerations, and braking acceleration (or deceleration) magnitudes that are dependent on several construction and safety factors. For instance, the most common types of passenger elevators are hydraulic, geared, gearless, and traction elevators. Typical lift accelerations range from 0.4 m/s^2 up to 1.2 m/s^2, with larger accelerations being required for higher rated speed elevators.[7]

The elevator used in the survey for this work was a hydraulic elevator constructed for low- to mid-rise buildings with an average maximum rated speed (v_m) of approximately 0.76 m/s.[8] As mentioned previously, the acceleration measured by the accelerometers is that experienced by the device, regardless of whether that force is due to gravity or not. Because the reported acceleration of the elevator exceeds the lower detection limit of either application used in this work by several orders of magnitude, the variations in acceleration caused by the elevator are measurable. The smartphone device was placed on the floor of the elevator with the *z*-component axis directed perpendicular to the floor, with the screen of the smartphone facing up. Because the elevator is confined to move only upwards and downwards and we assume that the direction of motion and F_g are exactly parallel, only the *z*-component of the acceleration was considered. The device recorded measurements as the elevator traveled upwards three floors, or a height change of approximately 14 m.

Figure 3 shows the results of the elevator exercise obtained by GraphicalGW [Fig. 3(a)] and Physics Toolbox Sensor Suite [Fig. 3(b)]. The left-most peak in both plots indicates the elevator is accelerating as it begins its ascent. While ascending, the smartphone device experiences a larger F_N as it opposes the direction of F_g, resulting in a larger *g*-force ratio and therefore larger acceleration (a_{peak}) than when the elevator is stationary (before the peak) or in constant velocity motion (not accelerating) after the peak. Conversely, the right-most trough in both plots indicates the elevator is decelerating as it approaches the destination. In this case, the smartphone device experiences a smaller F_N, resulting in a smaller *g*-force ratio and therefore smaller acceleration (a_{trough}) than when the elevator was in constant motion (not accelerating) before the trough or stationary after the trough.

The students should be required to calculate the accelerations of the elevator by applying the same elevation and latitude corrections to a_{peak} and a_{trough}, as follows:

$$a_{pcor} = a_{peak} - a_{lat} + a_{el} \tag{6}$$

$$a_{tcor} = a_{trough} - a_{lat} + a_{el}, \tag{7}$$

where a_{pcor} and a_{tcor} are the latitude and elevation corrected values of a_{peak} and a_{trough}, respectively. Note that even though the a_{lat} are the same in both Eqs. (6) and (7), the corresponding a_{el} differs because a_{trough} is measured an additional 14 m above the reference ellipsoid (251 m + 14 m = 265 m) relative to a_{peak} (251 m). Our results are given in Table II. The process of the elevator braking to come to a stop at the third floor has a lower value than when the elevator accelerates to ascend; however, braking occurs for a longer duration, with the practical application being a more comfortable arrival at the destination for passengers using the lift.

Table II. Results of the elevator accelerations using GraphicalGW and Physics Toolbox Sensor Suite on a smartphone device.

Application	a_{peak} (m/s^2)	a_{pcor} (m/s^2)	a_{trough} (m/s^2)	a_{tcor} (m/s^2)
GraphicalGW	10.91	1.09	9.09	-0.73
Physics Toolbox Sensor Suite	10.944	1.125	9.091	-0.726

Using a_{peak}, the rated speed of the elevator (v_{peak}) can be calculated and compared to v_m. Depending on students' mathematical backgrounds, the midpoint rule of the Riemann sum method can be used to approximate an integral to calculate the area under the peak. Alternatively, computational software can be used to perform a more accurate approximation. In either method, the data should be normalized to the stationary/non-acceleration horizontal trend. Since the elevator is initially stationary, v_{peak} calculated from integral approximations is directly comparable to v_m. For this exercise, we used Origin Lab 2019 plotting software to calculate the area under the ascent peak and determine v_{peak}, and our results are given in Table III.

Table III. Results of the velocities of the elevator using GraphicalGW and Physics Toolbox Sensor Suite on a smartphone device compared to the manufacturer[7] provided maximum velocity, v_m.

Application	v_{peak} (m/s)	v_m (m/s)[7]
GraphicalGW	0.8 ± 0.2	0.76
Physics Toolbox Sensor Suite	0.8 ± 0.2	

Lastly, it is possible to calculate the force necessary to support the elevator itself and the operator in the elevator, which can be calculated using Newton's second law:

$$F_S = ma + ma_{theory}, \tag{8}$$

where m is the mass of the elevator and the operator, and a is the acceleration of the elevator. When the elevator is accelerating, and its acceleration is positive, the support force is proportional to the sum of the elevator's acceleration and gravitational acceleration. On the other hand, when the elevator is decelerating, and its acceleration is negative, the support force is proportional to the difference between the elevator's acceleration and gravitational acceleration. The support force necessary to initially lift the elevator and operator is thus expected to be greater than that necessary to brake the elevator as it reaches a stop. For this example, we will assume the elevator and operator have a combined mass of 600 kg and use acceleration values determined using GraphicalGW. When the elevator is accelerating to ascend ($a = a_{pcor} = 1.09$ m/s^2), we obtain $F_S = 6.54 \times 10^3$ N. When the elevator is braking ($a = a_{tcor} = -0.73$ m/s^2), we obtain $F_S = 5.4 \times 10^3$ N.

Final remarks

The first exercise described here requires students to measure a_{grav} by observing their smartphone's acceleration while in free fall from any desired height using either the GraphicalGW and Physics Toolbox Sensor Suite applications. The results (Table I) agree well with a_{theory} at our latitude and elevation. The second exercise described here, an acceleration survey in an elevator, demonstrated that acceleration of an elevator during ascent and braking, as well as its rated speed, can be easily measured by both applications and agrees well with typical lift specifications, tabulated in Tables II and III. Accelerometers, rather than gravimeters, are suitable in this scientific demonstration as the determination of a_{grav} and the vertical acceleration of elevators does not require a device of high accuracy. The greater accuracy of the Physics Toolbox Sensor Suite application is apparent in the increased acquisition frequency during the experiment and in the number of significant digits displayed. In addition, the difference in acceleration at the basement and third floor might be caused by the difference in density of the material below the elevator shaft, which was not taken into consideration in this analysis. The increasing void region in the shaft below the elevator as the elevator ascends can be interpreted as a less dense region, which translates to a lower gravitational attraction than that at the lowest floor where no such void exists. Although the detection limits of the applications, as discussed in Part 1, are 0.01 m/s^2 for the GraphicalGW and 0.001 m/s^2 for the Physics Toolbox Sensor Suite, the standard deviations vary from 0.02 to 0.08 m/s^2 for the GraphicalGW and from 0.01 to 0.1 m/s^2 using the Physics Toolbox Sensor Suite, which limits their accuracy. Considering that Eq. (2) allows for variations in latitude to result in a change from 0.01 to 0.05 m/s^2 while Eq. (3) requires a minimum elevation gain of 3240 m to measure a change of 0.01 m/s^2, a field trip to a nearby location would generally not result in accurate measurements of elevation or latitude effects.

References

1. Meryem Berrada, Joshua A. H. Littleton, and Richard Secco, "Smartphones and gravitational acceleration I: Overview," *Phys. Teach.* **58**, 470 (Oct. 2020).
2. H. J. Götze, "International Gravity Formula," in H. K. Gupta, Encyclopedia of Solid Earth Geophysics. Encyclopedia of Earth Sciences Series (Springer, Dordrecht, 2011).
3. W. M. Telford, L. P. Geldart, and R. E. Sheriff, *Applied Geophysics*, 2nd ed. (Cambridge University Press, Cambridge, 1990), pp. 11–12.
4. W. Lowrie, *Fundamentals of Geophysics*, 2nd ed. (Cambridge University Press, Cambridge, 2007), pp. 43–105.
5. F. D. Stacey and P. M. Davis, *Physics of the Earth*, 4th ed. (Cambridge University Press, Cambridge, 2008), pp. 125-128.
6. H. Christian, S. Claessens, T. Fecher, M. Kuhn, R. Pail, and M. Rexer, "New ultrahigh-resolution picture of Earth's gravity field," *Geophys. Res. Lett.* **40**, 4279–4283 (Aug. 2013).
7. G. Barney and L. Al-Sharif, *Elevator Traffic Handbook*, 2nd ed. (Routledge Taylor & Francis Group, New York, 2016), pp. 87–112.
8. Thyssenkrupp Elevator Corporation, *Elevator Product Guide* (self-published online, 2019), pp. 22–23.

University of Western Ontario, London, ON, Canada; secco@uwo.ca